

Test of the Time-Dependent Mean-Field Theory in Kr-Induced Strongly Damped Collisions

K. T. R. Davies and V. Maruhn-Rezwani^(a)

Physics Division, Oak Ridge National Laboratory, Oak Ridge, Tennessee 37830

and

S. E. Koonin

W. K. Kellogg Radiation Laboratory, California Institute of Technology, Pasadena, California 91125

and

J. W. Negele

Center for Theoretical Physics, Department of Physics, Massachusetts Institute of Technology, Cambridge, Massachusetts 02139

(Received 5 June 1978)

Axially symmetric time-dependent mean-field calculations using a Skyrme-type effective interaction have been performed for $^{84}\text{Kr} + ^{208}\text{Pb}$ at $E_{\text{lab}} = 494$ MeV and $^{84}\text{Kr} + ^{209}\text{Bi}$ at $E_{\text{lab}} = 600$ MeV. Calculated fragment energies, mean masses, and scattering angles for strongly damped collisions are in good agreement with experiment, but mass distribution widths are an order of magnitude too small.

Although the time-dependent mean-field approximation is a conceptually appealing theory of large-amplitude nuclear dynamics,¹ computational considerations have previously restricted its application to collisions of light nuclei²⁻⁴ and the induced fission of the ^{236}U .⁵ While these calculations have had some success in reproducing experimental data,⁴ a new and potentially definitive test of the theory is its application to strongly damped heavy-ion collisions.⁶ For reactions such as $^{84}\text{Kr} + ^{208}\text{Pb}$ at $E_{\text{lab}} = 494$ MeV (Vandenbosch *et al.*⁷) and $^{84}\text{Kr} + ^{209}\text{Be}$ at $E_{\text{lab}} = 600$ MeV (Wolf and co-workers⁸) considered in this Letter, the strong side peaking of projectilelike fragments near the grazing angle, the energy loss associated with the deep inelastic peak, and the broad fragment-mass distribution centered about the initial partition place stringent demands on a microscopic theory having no free parameters.

Our time-dependent Hartree-Fock (TDHF) calculations evolve a set of axially symmetric single-particle wave functions in the mean-field generated by the finite-range Skyrme-type effective interaction of Ref. 5 with a rotational energy contribution,^{2,9} $L^2/2\mathcal{I}$, included in the intrinsic Hamiltonian. The coordinate-space TDHF methods of Ref. 2, 5, and 10 were used with the following modifications. The initial target and projectile wave functions were calculated assuming uniform fractional occupation of nonclosed spherical orbitals, and no pairing was included in either the static or dynamic calculations. The accuracy of our spatial mesh interval $\Delta x = 0.55$ fm was checked by verifying that in $^{40}\text{Ca} + ^{40}\text{Ca}$ collisions at the same center-of-mass energy per nucleon over the bar-

rier, doubling the discretization error by increasing Δx from 0.4 to 0.55 fm introduces errors of at most 4% in final kinetic energy loss and 8° in scattering angle. The moment of inertia, \mathcal{I} , is defined to be that of two point particles before the target-projectile density overlap reaches half nuclear-matter density, and the rigid-body value thereafter.⁹ Although studies of light systems at higher energies have indicated serious deficiencies in the axial-symmetry restriction, explicit comparisons using three-dimensional $^{40}\text{Ca} + ^{40}\text{Ca}$ calculations⁹ indicate that for the maximum center-of-mass energy per nucleon above the Coulomb barrier of 0.4 MeV considered in this work, the present approximations are adequate.

We have integrated the TDHF equations for the $^{84}\text{Kr} + ^{208}\text{Pb}$ system at six impact parameters and for the $^{84}\text{Kr} + ^{209}\text{Bi}$ system at ten impact parameters, obtaining two-fragment final states in each case. Although the absence of fused final states is consistent with a vanishing fusion cross section,¹¹ our calculations did not include the very smallest impact parameters. The Wilczyński plots in Figs. 1 and 2 indicate that the calculations quantitatively reproduce the overall behavior of the experimental data. In particular, the proper strong damping is found in the correct angular region, with many partial waves concentrating to give strong focusing in both angle and energy. As in classical calculations,⁶ the deflection functions shown in Fig. 3 indicate that the scattering angle is more forward than Rutherford scattering for angular momenta L just below grazing and then increases to 180° for small L .

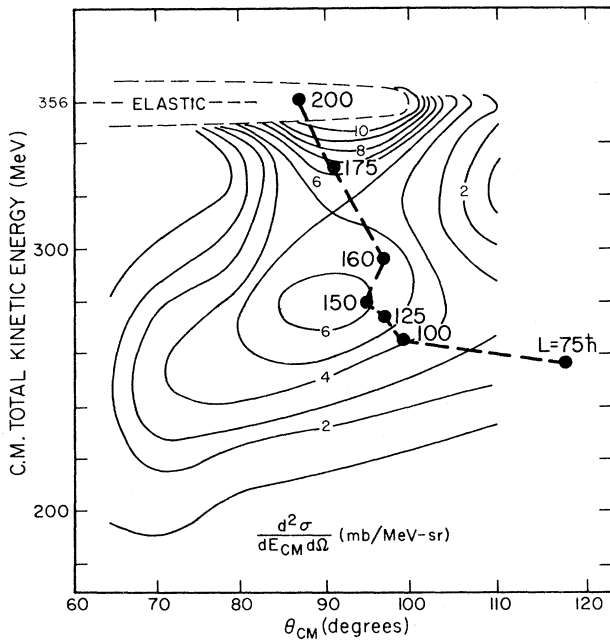


FIG. 1. Comparison of calculated points, labeled by the orbital angular momentum, with the experimental Wilczyński plot from Ref. 7 for $^{84}\text{Kr} + ^{208}\text{Pb}$ at $E_{\text{lab}} = 494$ MeV.

In the more energetic Kr + Bi system, an inner rainbow and a pronounced fluctuation arising from single-particle effects are also observed near $\theta_{\text{c.m.}} = 50^\circ$. Although the number of calculated impact parameters is insufficient to compute angular differential cross sections, it is clear that the deflection functions yield the proper experimental peak angles, θ_p . Note also that the much broader angular structure found experi-

mentally in the $\text{Kr} + \text{Bi}$ system is naturally reproduced by the calculation.

The contact time, τ , is defined as the interval during which the minimum density along the symmetry axis between the fragments exceeds one-half of nuclear matter density. As shown in Fig. 3, the contact time increases strongly with decreasing L . Thus, although smaller angular velocities are associated with the lower angular momenta, longer contact times cause the combined system to rotate through a larger angle. The $L = 180\hbar$ fluctuation in the Kr + Bi deflection function is then correlated with the unusually short contact time of this collision.

The final center-of-mass fragment total kinetic energy, $E_{k,\text{tot,c.m.}}$, decreases as L decreases, with nonperipheral collisions resulting in damping down to or below the experimental Coulomb barrier, independent of bombarding energy. Considered as a function of the contact time, τ , the energy loss increases monotonically, rapidly at first and then at a much slower rate, consistent with the behavior inferred from the experimental correlation between $E_{k,\text{tot,c.m.}}$ and the width of the fragment charge distribution.⁶

The deviation of the mean mass number of the Kr-like fragment from 84, $\Delta A = \bar{A} - 84$, and the full width at half-maximum of the fragment-mass distribution,¹² Γ_A , are displayed in Fig. 3. In the strongly damped region for Kr + Bi centered around a scattering angle of 50° , \bar{A} fluctuates around the observed value⁸ of 84. At very low impact parameters, \bar{A} increases significantly, although the calculated increase to roughly 90 at $\theta_{\text{c.m.}} = 85^\circ$ is of insufficient magnitude to agree

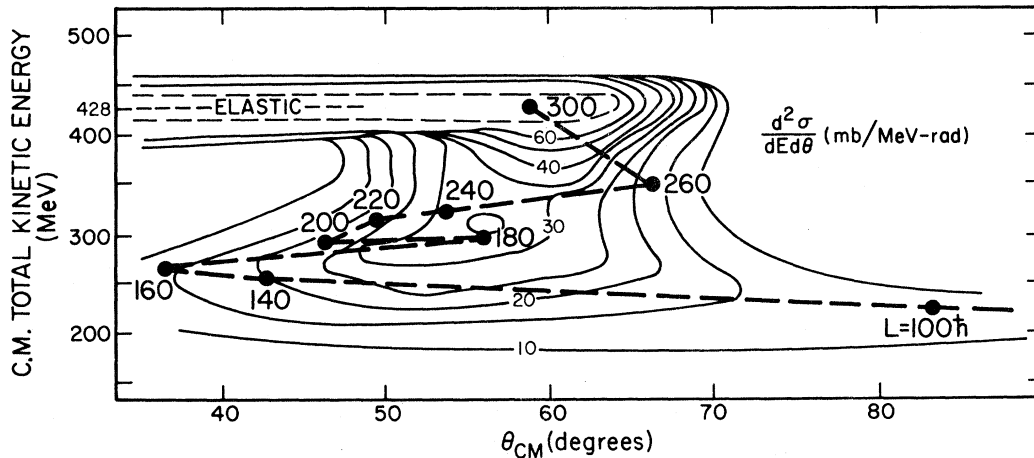


FIG. 2. Similar to Fig. 1 for $^{84}\text{Kr} + ^{208}\text{Bi}$ at $E_{\text{lab}} = 600$ MeV, with data from Ref. 8.

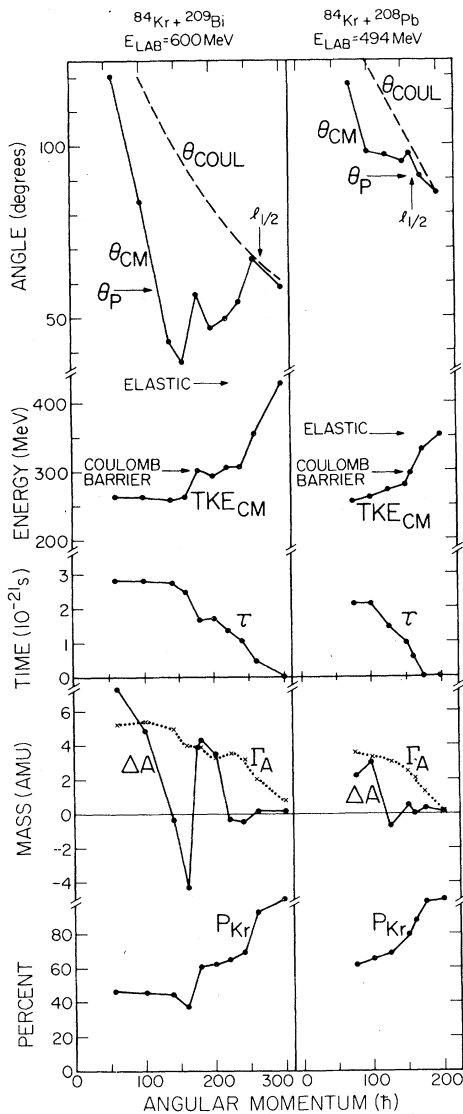


FIG. 3. Quantitative summary of TDHF results for Kr-induced collisions. Plotted as functions of the initial orbital angular momentum are $\theta_{c.m.}$, the final c.m. scattering angle; $E_{k, tot, c.m.}$, the final c.m. total kinetic energy of the fragments; τ , the contact time; ΔA , the net mass change of the light fragment; Γ_A , the full width at half-maximum of the mass distribution; and P_{Kr} , the percentage of Kr orbitals remaining in the light fragment after the collision. Also shown on the $\theta_{c.m.}$ graph are θ_{COUL} , the Rutherford deflection function; $l_{1/2}$, the angular momentum where the optical-model transmission coefficients fall to $\frac{1}{2}$ (Refs. 6 and 7); and θ_p , the peak angle in the experimental strongly damped angular distribution (Ref. 6). The Coulomb barriers indicated on the $E_{k, tot, c.m.}$ graphs correspond to point charges separated by 14.28 fm, the experimental (Ref. 6) strong-absorption radius for $^{84}\text{Kr} + ^{209}\text{Bi}$ at $E_{lab} = 600$ MeV.

with the experimental value⁸ of $\bar{A} = 110$. The width Γ_A is always an order of magnitude smaller than the observed value of roughly 50. The linear dependence of Γ_A^2 on τ is consistent with diffusion models, although the diffusion coefficients $\Gamma_A^2/16\tau \ln 2 = (0.5 \text{ and } 0.8 \text{ amu}^2)/(10^{-21} \text{ sec})$ for the Pb and Bi reactions are significantly small.

From the viewpoint of single-particle dynamics, the compound system consists of two slowly evolving time-dependent potential wells connected for a period of order 2×10^{-21} sec by a neck region through which single-particle orbitals freely pass at velocities up to the Fermi velocity, $(90 \text{ fm})/(10^{-21} \text{ sec})$. A single-particle, basis-dependent, but nevertheless instructive quantity is the fraction, P_{Kr} , of the initial Kr orbitals remaining in the final light fragment. As shown in Fig. 3, for strongly damped collisions there is substantial interchange of single-particle wave functions between the fragments, despite the fact that there is little net mass transfer. As in the model system studied in Ref. 1, dynamic resonances due to details of the specific single-particle wave functions in the neck region are to be expected. Indeed, the fluctuation in contact time for the Kr + Bi system $L = 180\hbar$ appears to be just such an effect, with detailed study of the time dependence of the nuclear density indicating that the short contact time arises from an unusually rapid depletion of density in the neck region and thus premature scission.

In summary, axially symmetric time-dependent mean-field calculations with no free parameters have been shown to account quantitatively for three essential features of Kr-induced strongly damped collisions: side-focusing at the appropriate angles, strong damping with the correct amount of energy loss, and small values of the net mass transfer. Their primary deficiency is the underestimation of the width of the fragment-mass distribution by an order of magnitude. Whether this discrepancy indicates a fundamental inadequacy of the mean-field approximation or arises from the axial-symmetry constraint in the present calculations remains an important question to be answered by further investigations of the type reported here.

Two of us (K.T.R.D. and V.M.R.) wish to acknowledge useful discussions with R. Cusson and H. Feldmeier. We are also grateful to J. Maruhn for providing a fast input/output code for the IBM 360 system. One of us (S.E.K.) acknowledges

receipt of an Alfred P. Sloan Foundation Fellowship. This work was supported in part by the National Science Foundation (PHY76-83685 and PHY77-21602) and the U. S. Department of Energy (EY-76-C-02-3069, *000). Oak Ridge National Laboratory is operated by Union Carbide Corporation for the U. S. Department of Energy.

^(a)Present address: Institut für Theoretische Physik, Universität Giessen, 6300 Giessen, West Germany.

¹P. Bonche, S. E. Koonin, and J. W. Negele, Phys. Rev. C **13**, 1226 (1976).

²S. E. Koonin, K. T. R. Davies, V. Maruhn-Rezwani, H. Feldmeier, S. J. Krieger, and J. W. Negele, Phys. Rev. C **15**, 1359 (1977).

³H. Flocard, S. E. Koonin, and M. S. Weiss, Phys. Rev. C **17**, 1682 (1978), references cited therein.

⁴P. Bonche, B. Grammaticos, and S. E. Koonin, Phys. Rev. C **17**, 1700 (1978).

⁵J. W. Negele, S. E. Koonin, P. Moller, J. R. Nix, and A. J. Sierk, Phys. Rev. C **17**, 1098 (1978).

⁶A thorough review of the general features of strongly damped collisions is contained in W. U. Schroder and J. R. Huizenga, Annu. Rev. Nucl. Sci. **27**, 465 (1977).

⁷R. Vandenbosch, M. P. Webb, and T. D. Thomas, Phys. Rev. C **14**, 143 (1976), and Phys. Rev. Lett. **36**, 459 (1976).

⁸K. L. Wolf, J. P. Unik, J. R. Huizenga, J. Birkelund, H. Freiesleben, and V. E. Viola, Phys. Rev. Lett. **33**, 1105 (1974); K. L. Wolf and C. T. Roche, in Proceedings of the Symposium on Macroscopic Features of Heavy-Ion Collisions, Argonne, Illinois, 1976, edited by D. G. Kovar, ANL Report No. ANL/PHY-76-2 (unpublished), Vol. I, p. 295.

⁹P. Hoodbhoy and J. W. Negele, Nucl. Phys. **A288**, 23 (1977).

¹⁰K. T. R. Davies, H. T. Feldmeier, M. S. Weiss, and H. Flocard, to be published. Our treatment of the relative orbital angular motion corresponds to prescription R2 of this reference.

¹¹J. Péter, C. Ngô, and B. Tamain, Nucl. Phys. **A250**, 351 (1975).

¹²For pure Slater determinants, the formulation of Ref. 1 can be used to compute the width of the fragment mass distribution, $\Gamma_A^2 = 8 \ln 2 \text{tr}[\rho - \rho^2]$, where ρ is the density matrix for the light fragment. This expression can be extended for use with the filling approximation by ignoring nonlinearities in the evolution and appropriately averaging the final widths of all determinants present in the initial wave function.

Observation of the α -Particle Breakup Process at $E_\alpha^{\text{lab}} = 172.5$ MeV

A. Budzanowski,^(a) G. Baur, C. Alderliesten,^(b) J. Bojowald, C. Mayer-Böricke, W. Oelert, and P. Turek
Institut für Kernphysik der Kernforschungsanlage Jülich, D-517 Jülich, West Germany

and

F. Rösel and D. Trautmann
Institut für Theoretische Physik, Universität Basel, CH-4056 Basel, Switzerland
(Received 21 March 1978)

Double-differential cross sections $d^2\sigma/d\Omega dE$ have been measured for the (α , ^3He) reaction on Ni isotopes at $E_\alpha^{\text{lab}} = 172.5$ MeV. A distinct peak was found, having a half-width of ~ 40 MeV and a strongly decreasing intensity with increasing reaction angle. Theoretical evidence is provided to attribute this peak to the (α , ^3He) stripping process into the continuum.

In connection with preequilibrium reaction theories, there has been growing interest in the study of continuous spectra of particles emitted in nuclear reactions. In the present investigation spectra of ^3He particles emitted in reactions induced by 172.5-MeV α particles on $^{58,60,62,64}\text{Ni}$ targets have been studied in the energy range from 50 to 160 MeV (lab). The experiment has been performed at the Jülich isochronous cyclotron JULIC in a 100-cm-diam scattering chamber. Two ΔE - E semiconductor telescopes were used,

each consisting of a 1000- μm -thick commercial Si surface-barrier ΔE transmission detector and a Li-drifted Ge E detector of the side-entry type developed in the detector laboratory of the institute.¹

In addition to the peaks corresponding to stripping to bound states (neutron transfer), the ^3He spectra show at forward angles a broad peak with a half-width of ≈ 40 MeV and which is centered around $E_{^3\text{He}}^{\text{c.m.}} = 122$ MeV (Fig. 1). Its intensity decreases by orders of magnitude with increasing